

Loss Of Load Probability Analysis For Cellular Network Transceiver Base Station Solar Pv Power System

Usah, Emmamuel Okon

Department of Physics, University of Uyo

Abstract—In this paper, loss of load probability analysis for cellular network transceiver base station solar PV power system is presented. The daily load demand for the case study cellular network transceiver base station is 48252 Wh/day. The daily load demand and the solar radiation data are used in PVSyst to select the requisite PV system components sizes and also to determine the loss of load probability and loss of load duration. Particularly, the study focused on providing detailed insight into the exact day and time that loss of load will occur in each month based on PVSyst simulation results. The results showed that there is a total annual average loss of load probability (LOLP) of 9% with a total annual loss of load duration of 792 hours per year. The results show that the loss of load occurred on 30th of January and it lasted for 10 hours, from about 2 am to 12 noon. Also, the results show that the loss of load occurred on two consecutive days in March, namely, on 12th and 13th of March and it lasted for 31 hours, from about 6 am on 12th of March to 1pm on 13th of March. Furthermore, the highest loss of load duration occurred in the month of July with about 169 hours of no power supply to the load. This amounts to about 7.041667 days of power outage. The idea presented in this paper can be employed to determine the exact time that loss of load can occur all through the year. This will help in power system planning.

Keywords— Loss Of Load Probability, Solar PV Power System Cellular Network, Daily Load Demand, Transceiver Base Station, PVSyst Software

1. INTRODUCTION

Cellular network is the fundamental technology employed in mobile phones and other wireless networking and personal communication systems [1,2,3,4,5,6,7,8,9,10]. Basically, cellular network consist of at least a fixed-location transceiver base station which provides connectivity to the various communication devices that are with the coverage area of the base station [11,12,13,14,15,16,17]. Notably, the coverage area is divided into different cells, where neighboring cell are designed to operate at different frequencies [18,19,20,21,22,23,24,25,26]. In practice, the base station is usually a critical equipment in cellular networks because the failure of the base station amounts to the failure communication for the devices that are within the coverage area of the base station [27,28,29,30,31]. One of the dominant causes of failure of the cellular network base station is electric power failure.

In some cases, the base stations are located in remote areas that do not have access to the electric power from the national grid. In other cases, the national grid do not supply power regularly, or the power supplied from the grid are not good enough to power the base station equipment. In such cases, alternative power supply is required. One of the performance measures of such PV power system is the loss of load probability (LOLP). The LOLP defines the fraction of time that the load demand could not be satisfied over a given period. In this paper, the loss of load probability for a cellular network transceiver base station powered by a standalone PV power system is presented. The study seek to estimate the exact day in a year and the exact time and duration in each of those days when power failure will be experienced at the base station. The study is essential for power generation planning and load shading management system at the base station. The mathematical details are presented along with numerical example based on a case study transceiver base station. The analysis is simulated using PVSyst software.

2 METHODOLOGY

When the power source fails to generate enough power to meet the load demand, there will be a power failure or loss of load. Loss of Load Probability (LOLP) gives a measure of power failure incidence and the fraction of the period which the power failure occurred due to insufficient power generation from the power source. Generally, LOLP can be computed from the knowledge of the daily energy yield of the power source and the daily energy demand. In this paper, the power source is a PV solar power system. For PV solar power system, over a period of N days, the daily PV energy yield (E_{pvd}) for day j (where j = 1, 2, 3...N) is computed as follows;

$$E_{pvd(j)} = (A_{pv})(G_{av(j)})(\eta_{pv})(\eta_{wire})(\eta_{inv}) \quad (1)$$

Where, A_{pv} represents the PV-array area; G_{av} represents the solar radiation incident on the PV-array for day j; represents the PV array efficiency which is about 18.54% or 0.185; η_{wire} represents the wire efficiency (0.95); and η_{inv} represents the efficiency (0.9). Let the daily load demand for day j be denoted as $E_{L(j)}$, then energy difference $E_{d(j)}$ on day j is computed as;

$$E_{d(j)} = E_{pv(j)} - E_{L(j)} \quad (2)$$

The annual energy difference, $E_{Y(j)}$ is computed as;

$$E_{Y(j)} = \sum_{j=1}^{365} (E_{pv(j)} - E_{L(j)}) \quad (3)$$

When $E_{d(j)}$ is positive, then there is Energy Excess ($EX_{d(j)}$). The excess energy is used to charge the battery bank, hence the Energy Excess ($EX_{d(j)}$) is stored in battery bank.

$$EX_{d(j)} = E_{d(j)} \text{ for } E_{pv(j)} \geq E_{L(j)} \quad (4)$$

When $E_{d(j)}$ is negative, then there is Energy Deficit ($ED_{d(j)}$). The energy stored in the battery bank is then used to supply the energy to the load.

$$ED_{d(i)} = E_{d(j)} \text{ for } E_{pv(j)} < E_{L(j)} \quad (5)$$

Loss of Load Probability (LOLP) over a period of one year is the ratio of total annual energy deficit to the total annual energy demand, where,

$$LOLP = \frac{\sum_{j=1}^{365} (ED_{d(i)})}{\sum_{j=1}^{365} (E_{L(j)})} \quad (6)$$

Loss of Load Probability (LOLP) over a period of N days is the ratio of total energy deficit to the total energy demand over the period of N days, where,

$$LOLP = \frac{\sum_{j=1}^N (ED_{d(i)})}{\sum_{j=1}^N (E_{L(j)})} \quad (7)$$

Also, Loss of Load Probability (LOLP) can be computed in terms of the ratio of the total power failure time over a given period to the total time in the period. For instance, the ratio of the total power failure hours in a year to the total number of hours in a year gives the LOLP in a year.

$$LOLP = \frac{\text{Power failure time}}{\text{Total period of time}} \quad (8)$$

The load demand for the cellular network transceiver base station is given Table 1 with a daily load of 48252 Wh/day.

Table 1 The load demand for the cellular network transceiver base station

S/N	THE EQUIPMENT	QTY	POWER RATING (W)	DURATION (h)	ENERGY DEMAND/DAY (Wh)
1	Base Transceiver System (BTS)	2	50	24	2160
2	Air Conditioner	2	1120	12	26856
3	Security light	3	160	12	5760
4	Fluorescent lamp	4	30	0.3	36
5	Aviation warning light	5	160	12	9600
6	Incandescent bulb	3	60	12	2160
7	Connecting Microwave	1	70	24	1680
Total Daily Energy Demand (Wh)					48252

The solar radiation and ambient temperature data for the study site are given in Table 2. The scatter plot of the daily solar radiation data on the horizontal plane for study site is shown in Figure 2.

3. RESULTS AND DISCUSSION

The load demand and solar radiation data are used in PVSyst to select the requisite PV system components sizes and also determine the loss of load probability and loss of load duration. The schematic diagram of the PV power system is given in Figure 3, the simulation parameters are presented in Figure 4 and the results on energy use and loss of load are presented in Table 3 while the graph plot of the results on the monthly loss of load duration is presented in Figure 5. The results in Table 3 shows that there is a total annual average loss of load probability (LOLP) of 9% with a total annual loss of load duration of 792 hours per year. In essence, out of the 8760 hours in a year, there is no energy supplied to the load for a total of 792 hours in a year. This amounts to annual $LOLP = \left(\left(\frac{792}{8760} \right) 100\% \right) = 9.04109589\% \approx 9\%$, as shown in Table 3.

Table 2 The solar radiation and ambient temperature data for the study site

Interval beginning	GlobHor kWh/m².mth	GlobInc kWh/m².mth	T Amb °C
January	165.2	184.9	26.00
February	149.2	153.8	26.40
March	160.9	151.9	26.30
April	151.5	132.2	26.40
May	141.1	112.1	26.30
June	112.5	93.4	25.60
July	102.3	84.7	24.80
August	117.8	101.5	24.40
September	109.5	100.8	24.70
October	132.1	129.8	25.10
November	149.1	162.3	25.40
December	159.0	180.5	25.70
Year	1650.2	1587.9	25.59

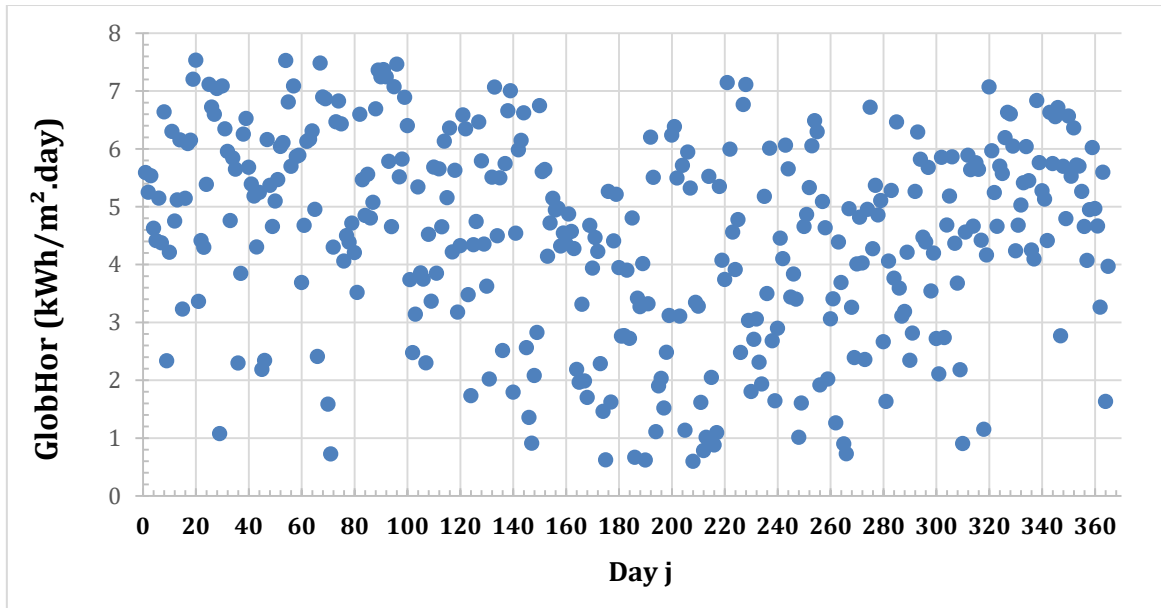


Figure 2 Scatter plot of the daily solar radiation data on the horizontal plane

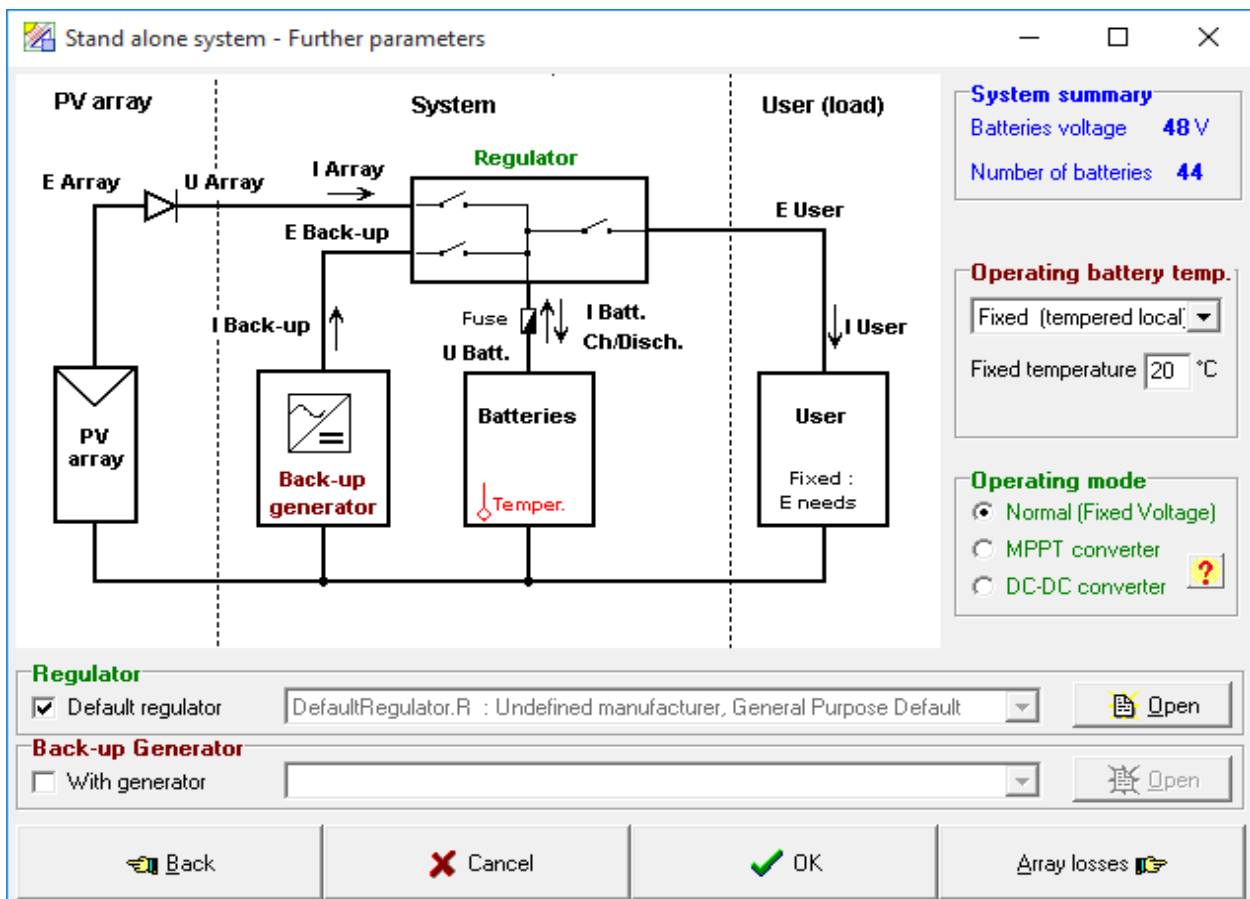


Figure 3 The schematic diagram of the PV Power System

PVSYST V5.20		31/05/21		Page 1/4	
Stand Alone System: Simulation parameters					
Project : LOLP BASE STATION					
Geographical Site		SOUTH SOUTH AKWA IBOM		Country Nigeria	
Situation		Latitude 5.0°N		Longitude 5.0°E	
Time defined as		Legal Time Time zone UT+1		Altitude 56 m	
Meteo data :		SOUTH SOUTH AKWA IBOM from NASA-SSE, Synthetic Hourly data			
Simulation variant : New simulation variant					
		Simulation date		31/05/21 08h00	
Simulation parameters					
Collector Plane Orientation		Tilt 0°		Azimuth 0°	
PV Array Characteristics					
PV module		SI-poly Model Quick Tile D4-FrP148			
		Manufacturer Sesol			
Number of PV modules		In series 9 modules		In parallel 43 strings	
Total number of PV modules		Nb. modules 387		Unit Nom. Power 48 Wp	
Array global power		Nominal (STC) 19 kWp		At operating cond. 17 kWp (50°C)	
Array operating characteristics (50°C)		U mpp 57 V		I mpp 291 A	
Total area		Module area 200 m²			
PV Array loss factors					
Thermal Loss factor		Uc (const) 20.0 W/m²K		Uv (wind) 0.0 W/m²K / m/s	
=> Nominal Oper. Coll. Temp. (G=800 W/m², Tamb=20°C, Wind velocity = 1m/s.)				NOCT 56 °C	
Wiring Ohmic Loss		Global array res. 3.3 mOhm		Loss Fraction 1.5 % at STC	
Module Quality Loss				Loss Fraction 2.5 %	
Module Mismatch Losses				Loss Fraction 4.0 % (fixed voltage)	
Incidence effect, ASHRAE parametrization		IAM = 1 - bo (1/cos I - 1)		bo Parameter 0.05	
System Parameter		System type		Stand Alone System	
Battery		Model		Dural 3C	
		Manufacturer		Electrona	
Battery Pack Characteristics		Voltage 48 V		Nominal Capacity 1100 Ah	
		Nb. of units		4 in series x 11 in parallel	
		Temperature		Fixed (20°C)	
Regulator		Model		General Purpose Default	
		Technology		Undefined	
Battery Management Thresholds		Charging 54.7/52.3 V		Temp coeff. -5.0 mV/°C/elem.	
		Back-Up Genset Command 47.3/51.6 V		Discharging 47.0/50.4 V	
User's needs :		Daily household consumers average		Constant over the year 48 kWh/Day	

Figure 4 The simulation parameters

Table 3 The results on energy use and loss of load

**New simulation variant
 Energy Use**

	EArray	E Load	E User	SolFrac	T LOL	Pr LOL
	kWh	kWh	kWh		Hour	%
January	1882	1496	1476	0.987	10	1.3
February	1701	1351	1326	0.982	12	1.8
March	1838	1496	1432	0.958	31	4.2
April	1784	1448	1437	0.992	5	0.7
May	1661	1496	1332	0.890	81	10.9
June	1377	1448	1238	0.855	104	14.5
July	1277	1496	1156	0.773	169	22.8
August	1436	1496	1163	0.778	165	22.2
September	1374	1448	1223	0.845	112	15.6
October	1653	1496	1393	0.931	51	6.9
November	1710	1448	1367	0.944	40	5.6
December	1839	1496	1477	0.988	9	1.3
Year	19532	17612	16020	0.910	792	9.0

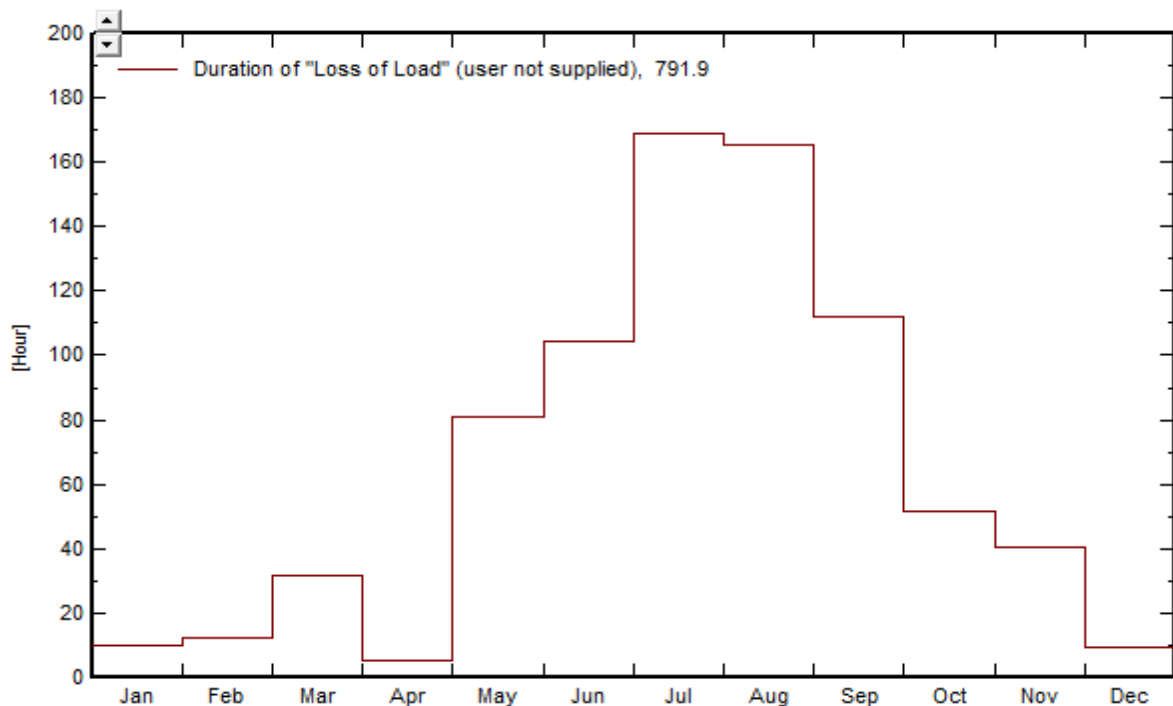


Figure 5 The Monthly Loss of Load Duration

The bar chart of the energy demand (load) and energy supplied by the PV to the load for the month of January are presented in Figure 6. Also, the graph plot of exact day loss of load occurred in the month of January is shown in Figure 7 while the graph plot showing of the exact time and duration of loss of load in the month of January is given in Figure 8. The results in Figure 6, Figure 7 and Figure 8 show that the loss of load occurred on 30th of January and it lasted for 10 hours, from about 2 am to 12 noon.

The bar chart of the energy demand (load) and energy supplied by the PV to the load for the month of March are presented in Figure 9. Also, the graph plot of exact day loss of load occurred in the month of March is shown in Figure 10 while the graph plot showing of the exact time and duration of loss of load in the month of March is given in Figure 11. The results in Figure 9, Figure 10 and Figure 11 show that the loss of load occurred on two consecutive days in March, namely, on 12th and 13th of March and it lasted for 31 hours, from about 6 am on 12th of March to

1pm on 13th of March. Similar approach can be used to evaluate the details of the loss of load probability for the rest of the months. The highest loss of load duration occurred in the month of July with about 169 hours of no

power supply to the load. This amounts to about 7.041667 days of power outage.

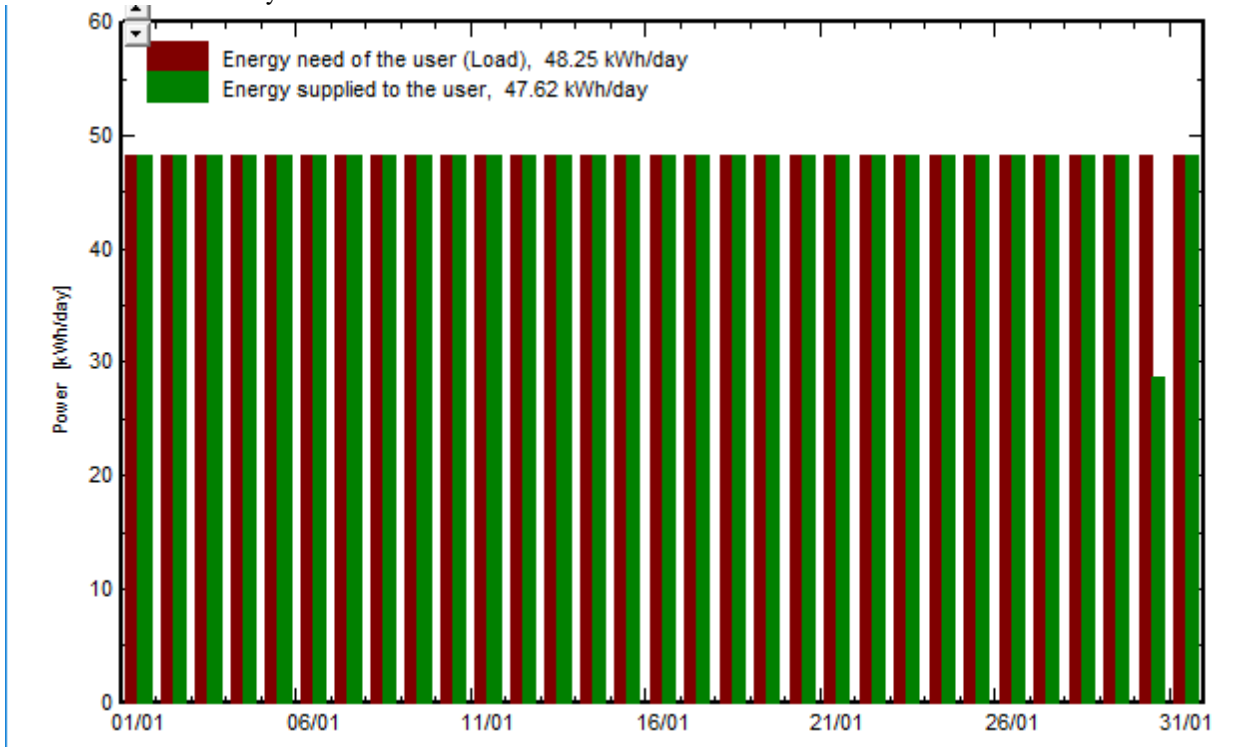


Figure 6 The energy demand (load) and energy supplied by the PV to the load for the month of January

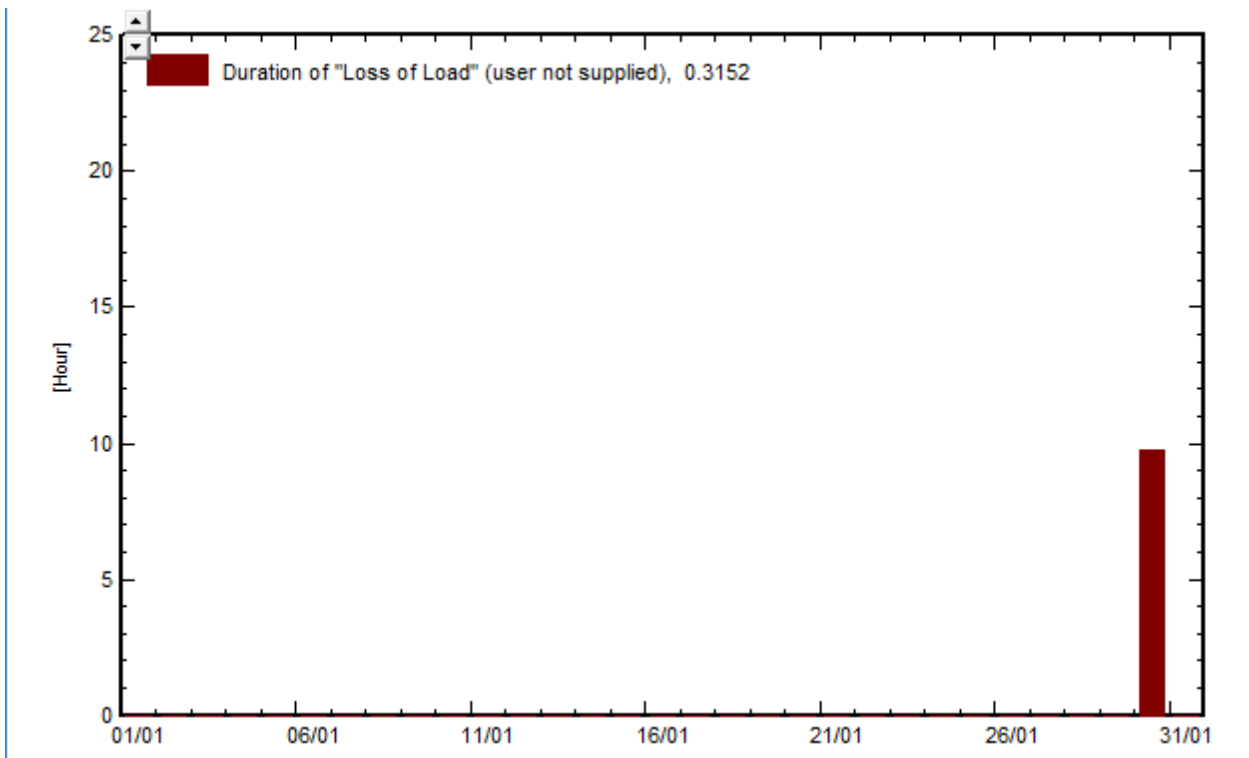


Figure 7 The plot of exact day loss of load occurred in the month of January

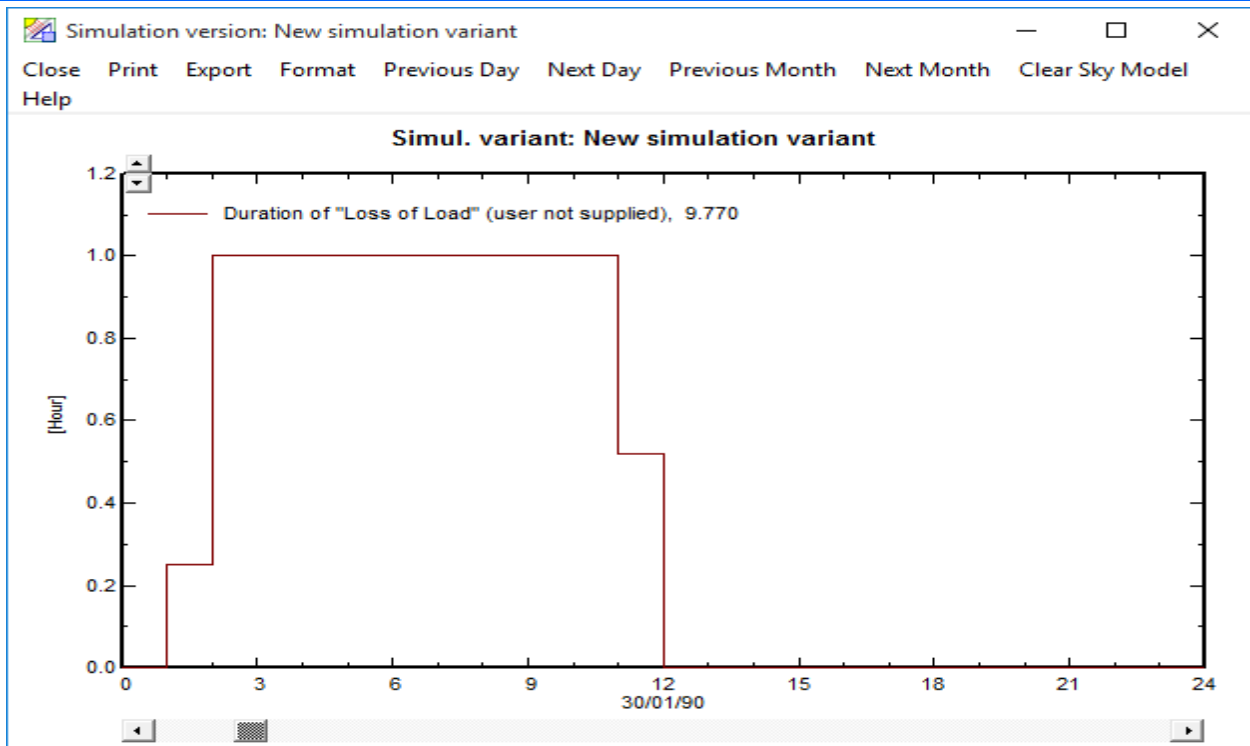


Figure 8 The plot of the exact time and duration of loss of load in the month of January

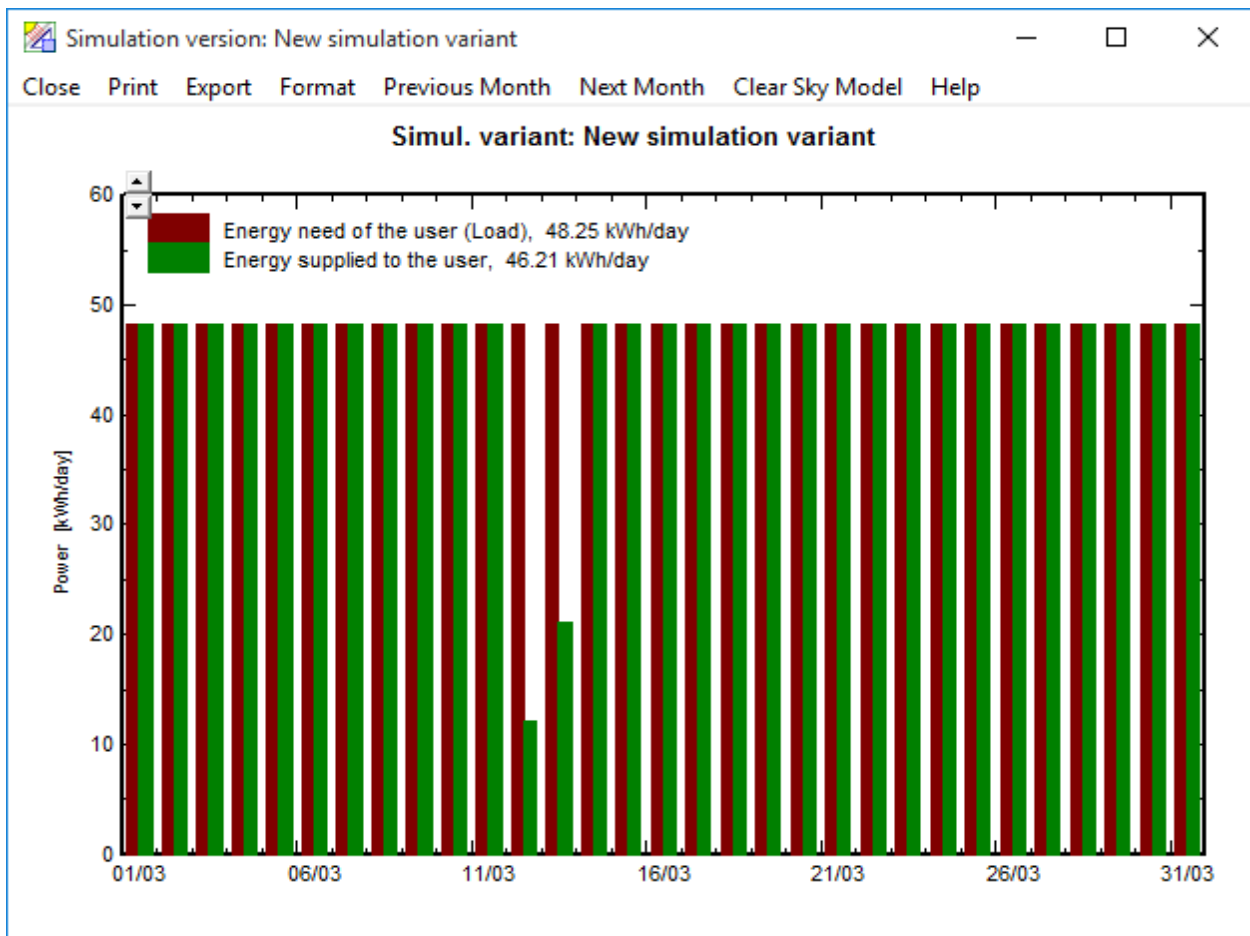


Figure 9 The energy demand (load) and energy supplied by the PV to the load for the month of March

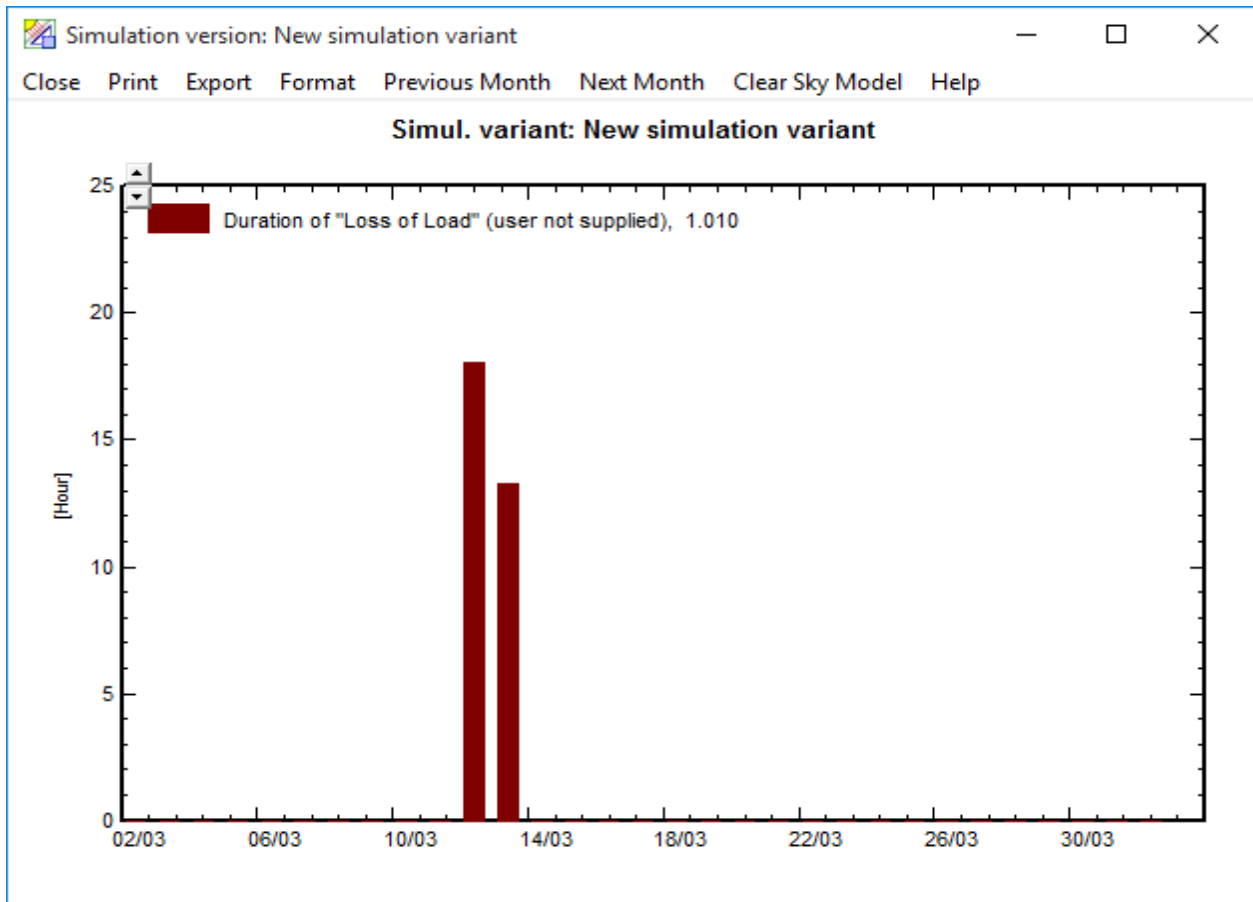


Figure 10 The plot of exact day loss of load occurred in the month of March

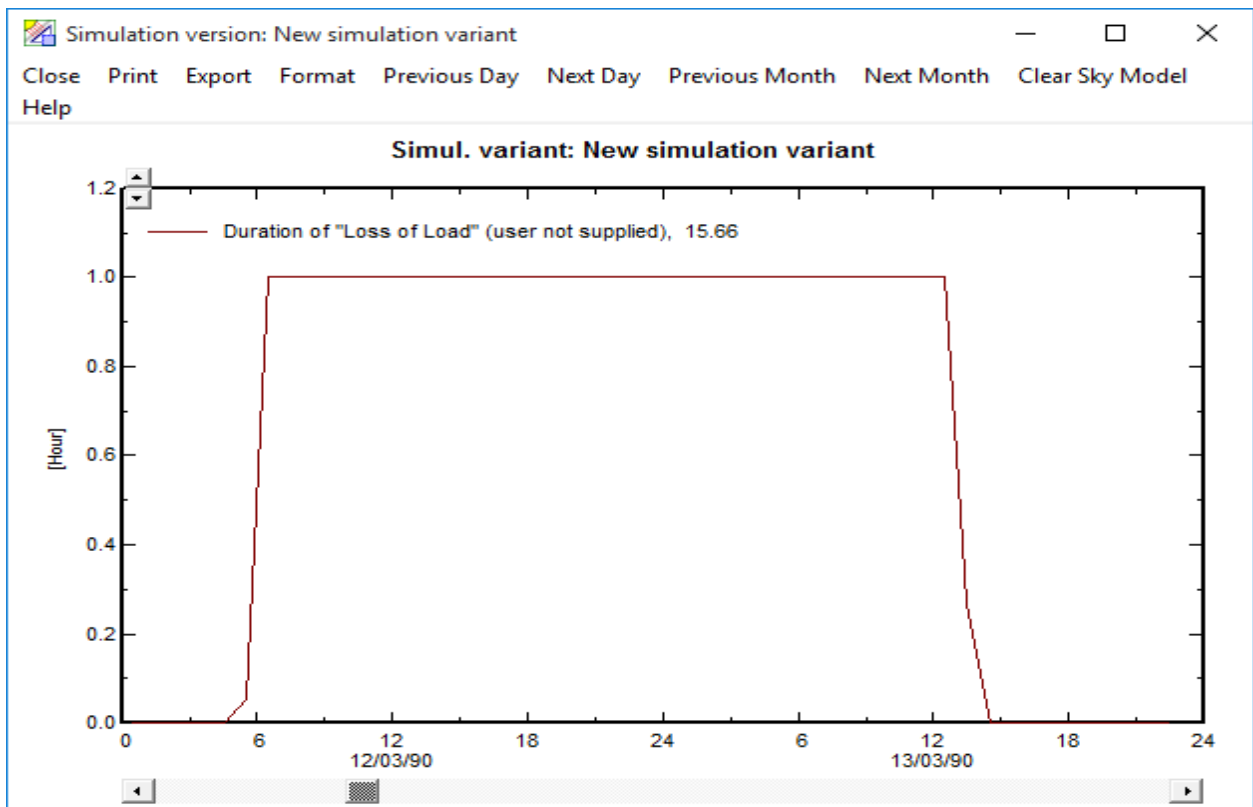


Figure 11 The plot of the exact time and duration of loss of load in the month of March

4. CONCLUSION

Analysis of the loss of load probability and loss of load duration for a standalone PV power system is presented. The study used a cellular network transceiver base station as the load. The study seeks to provide detailed insight into the exact day and time the loss of load will occur in each month based on the PVSyst simulation results. The results of the monthly and annual loss of load probability and loss of load duration are presented. Also, the exact day and time the loss of load occurred in the months of January and March are presented. Similar approach can be employed to determine the exact time the loss of load can occur all through the year. This will help in power system planning.

REFERENCES

1. Yang, P., Xiao, Y., Xiao, M., & Li, S. (2019). 6G wireless communications: Vision and potential techniques. *IEEE Network*, 33(4), 70-75.
2. Wang, S., & Ran, C. (2016). Rethinking cellular network planning and optimization. *IEEE Wireless Communications*, 23(2), 118-125.
3. Li, Y., Peng, C., Yuan, Z., Li, J., Deng, H., & Wang, T. (2016, October). Mobileinsight: Extracting and analyzing cellular network information on smartphones. In *Proceedings of the 22nd Annual International Conference on Mobile Computing and Networking* (pp. 202-215).
4. Abboud, K., Omar, H. A., & Zhuang, W. (2016). Interworking of DSRC and cellular network technologies for V2X communications: A survey. *IEEE transactions on vehicular technology*, 65(12), 9457-9470.
5. Zhang, X., & Andrews, J. G. (2015). Downlink cellular network analysis with multi-slope path loss models. *IEEE Transactions on Communications*, 63(5), 1881-1894.
6. Deng, N., Zhou, W., & Haenggi, M. (2015). Heterogeneous cellular network models with dependence. *IEEE Journal on selected Areas in Communications*, 33(10), 2167-2181.
7. Chinchali, S., Hu, P., Chu, T., Sharma, M., Bansal, M., Misra, R., ... & Katti, S. (2018, April). Cellular network traffic scheduling with deep reinforcement learning. In *Proceedings of the AAAI Conference on Artificial Intelligence* (Vol. 32, No. 1).
8. Yang, A. M., Yang, X. L., Chang, J. C., Bai, B., Kong, F. B., & Ran, Q. B. (2018). Research on a fusion scheme of cellular network and wireless sensor for cyber physical social systems. *IEEE Access*, 6, 18786-18794.
9. Miyoshi, N., & Shirai, T. (2014). A cellular network model with Ginibre configured base stations. *Advances in Applied Probability*, 46(3), 832-845.
10. Malandrino, F., Chiasserini, C. F., & Kirkpatrick, S. (2017). Cellular network traces towards 5G: Usage, analysis and generation. *IEEE Transactions on Mobile Computing*, 17(3), 529-542.
11. Alsharif, M. H., Nordin, R., & Ismail, M. (2015). Energy optimisation of hybrid off-grid system for remote telecommunication base station deployment in Malaysia. *EURASIP Journal on Wireless Communications and Networking*, 2015(1), 1-15.
12. Ding, G., Wang, J., Wu, Q., Yao, Y. D., Song, F., & Tsiftsis, T. A. (2015). Cellular-base-station-assisted device-to-device communications in TV white space. *IEEE Journal on Selected Areas in Communications*, 34(1), 107-121.
13. Maamari, D., Devroye, N., & Tuninetti, D. (2016). Coverage in mmWave cellular networks with base station co-operation. *IEEE transactions on Wireless Communications*, 15(4), 2981-2994.
14. Qian, L. P., Wu, Y., Zhou, H., & Shen, X. (2017). Joint uplink base station association and power control for small-cell networks with non-orthogonal multiple access. *IEEE Transactions on Wireless Communications*, 16(9), 5567-5582.
15. Lee, S., Lee, S., Kim, K., & Kim, Y. H. (2015). Base station placement algorithm for large-scale LTE heterogeneous networks. *PLoS one*, 10(10), e0139190.
16. Barazzetta, M., Micheli, D., Bastianelli, L., Diamanti, R., Totta, M., Obino, P., ... & Primiani, V. M. (2017). A comparison between different reception diversity schemes of a 4G-LTE base station in reverberation chamber: a deployment in a live cellular network. *IEEE Transactions on Electromagnetic Compatibility*, 59(6), 2029-2037.
17. Ding, M., & Lopez-Perez, D. (2017). Performance impact of base station antenna heights in dense cellular networks. *IEEE Transactions on Wireless Communications*, 16(12), 8147-8161.
18. Lee, D., Zhou, S., Zhong, X., Niu, Z., Zhou, X., & Zhang, H. (2014). Spatial modeling of the traffic density in cellular networks. *IEEE Wireless Communications*, 21(1), 80-88.
19. Mishra, S., & Mathur, N. (2014). Load balancing optimization in LTE/LTE-A cellular networks: a review. *arXiv preprint arXiv:1412.7273*.
20. ElBamby, M. S., Bennis, M., Saad, W., & Latva-Aho, M. (2014, August). Dynamic uplink-downlink optimization in TDD-based small cell networks. In *2014 11th International*

- Symposium on Wireless Communications Systems (ISWCS)* (pp. 939-944). IEEE.
21. Bai, T., Alkhateeb, A., & Heath, R. W. (2014). Coverage and capacity of millimeter-wave cellular networks. *IEEE Communications Magazine*, 52(9), 70-77.
 22. Goyal, S., Liu, P., Panwar, S. S., Difazio, R. A., Yang, R., & Bala, E. (2015). Full duplex cellular systems: will doubling interference prevent doubling capacity?. *IEEE Communications Magazine*, 53(5), 121-127.
 23. Wu, Q., Li, G. Y., Chen, W., Ng, D. W. K., & Schober, R. (2017). An overview of sustainable green 5G networks. *IEEE Wireless Communications*, 24(4), 72-80.
 24. Pedersen, K. I., Berardinelli, G., Frederiksen, F., Mogensen, P., & Szufarska, A. (2016). A flexible 5G frame structure design for frequency-division duplex cases. *IEEE Communications Magazine*, 54(3), 53-59.
 25. Mishra, S., & Mathur, N. (2014). Load balancing optimization in LTE/LTE-A cellular networks: a review. *arXiv preprint arXiv:1412.7273*.
 26. Xu, F., Lin, Y., Huang, J., Wu, D., Shi, H., Song, J., & Li, Y. (2016). Big data driven mobile traffic understanding and forecasting: A time series approach. *IEEE transactions on services computing*, 9(5), 796-805.
 27. Bor-Yaliniz, R. I., El-Keyi, A., & Yanikomeroglu, H. (2016, May). Efficient 3-D placement of an aerial base station in next generation cellular networks. In *2016 IEEE international conference on communications (ICC)* (pp. 1-5). IEEE.
 28. Giordani, M., Mezzavilla, M., & Zorzi, M. (2016). Initial access in 5G mmWave cellular networks. *IEEE Communications Magazine*, 54(11), 40-47.
 29. Azharuddin, M., Kuila, P., & Jana, P. K. (2015). Energy efficient fault tolerant clustering and routing algorithms for wireless sensor networks. *Computers & Electrical Engineering*, 41, 177-190.
 30. Desai, V., Krzymien, L., Sartori, P., Xiao, W., Soong, A., & Alkhateeb, A. (2014, November). Initial beamforming for mmWave communications. In *2014 48th Asilomar Conference on Signals, Systems and Computers* (pp. 1926-1930). IEEE.
 31. Younis, M., Senturk, I. F., Akkaya, K., Lee, S., & Senel, F. (2014). Topology management techniques for tolerating node failures in wireless sensor networks: A survey. *Computer Networks*, 58, 254-283.